ISBN: 978-3-95450-232-5 ISSN: 2673-7000 doi:10.18429/JACoW-NAPAC2022-MOPA50

INTEGRATED PHOTONICS STRUCTURE CATHODES FOR LONGITUDINALLY SHAPED BUNCH TRAINS

S. J. Coleman*, D. Abell, C. Hall, RadiaSoft LLC, Boulder, CO, USA
S.-Y. Kim, P. Piot, J. Power, Argonne National Laboratory, Lemont, IL, USA
R. Kapadia, University of Southern California, Los Angeles, CA, USA
S. Karkare, Arizona State University, Tempe, AZ, USA

Abstract

Compact, high-gradient structure wakefield accelerators can operate at improved efficiency using shaped electron beams, such as a high transformer ratio beam shape, to drive the wakes. These shapes have generally come from a photocathode gun followed by a transverse mask to imprint a desired shape on the transverse distribution, and then an emittance exchanger (EEX) to convert that transverse shape into a longitudinal distribution. This process discards some large fraction of the beam, limiting wall-plug efficiency as well as leaving a solid object in the path of the beam. In this paper, we present a proposed method of using integrated photonics structures to control the emission pattern on the cathode surface. This transverse pattern is then converted into a longitudinal pattern at the end of an EEX. This removes the need for the mask, preserving the total charge produced at the cathode surface. We present simulations of an experimental set-up to demonstrate this concept at the Argonne Wakefield Accelerator.

INTRODUCTION

Beam-driven structure wakefield accelerators – either dielectric wakefield accelerators or structures made using metamaterials – are a promising path for ~1 GV m^{-1} accelerating gradients for high energy lepton colliders or X-ray free-electron lasers [1–3]. Achieving an efficient transfer of energy from the drive beam to the witness beam requires specially shaped bunches to achieve a high transformer ratio. These shapes have been achieved [4, 5] using a transverse intercepting mask followed immediately by an emittance exchange beamline (EEX) [6]. While this technique produces the desired longitudinal current distribution to achieve high transformer ratios, the masks discard up to 80% of the bunch charge [7]. This limits the wall-plug efficiency available for these accelerators. A technique which would eliminate the need for the mask would restore the efficiency and introduce new flexibility in structure shaping. In one approach nano-engineered field emission arrays coupled with EEX have been shown to generate bunchlets with spacing as small as 13 nm [8].

We describe a configuration which uses integrated photonics structures (IPS) to shape the transverse profile on the photocathode surface, and transport that engineered shape through the EEX with no substantial loss of initial bunch charge. We propose to generate a horizontal bunchlet comb whose centroids become, after emittance exchange, a longitudinal bunchlet comb suitable for driving a terahertz dielectric wakefield accelerator.

This technique would reduce requirements on laser and rf power at fixed final bunch charge, or enable substantially higher final bunch charge at fixed power requirements. The technique is also extremely flexible – although we will focus on resonant wakefield excitation [9, 10].

THEORY

Emittance Exchange (EEX) is a tool to manipulate the phase space of a beam, shaping the downstream longitudinal properties by controlling the upstream transverse properties.

The EEX beamline at the Argonne Wakefield Accelerator (AWA) considered throughout this paper consists of a double-dogleg where a transverse deflecting cavity (TDC) is positioned between two identical doglegs, a configuration that provides an exact emittance exchange [11]. A TDC is an rf cavity operating in dipole mode, and has a longitudinal electric field with a spatially-varying gradient, such that the field strength varies linearly with transverse distance from the axis. We specifically consider the AWA EEX beamline parameters for which the TDC is a 1.3-GHz RF cavity operating on the $\mathrm{TM}_{110,\pi}$ mode [12]. Placement of the TDC in a dispersive region at the center of the double-dogleg, and careful selection of the TDC voltage and rf wavelength relative to the dogleg dispersion, enables complete exchange of the horizontal and longitudinal phase space coordinates [6]. The bunch evolves as

$$(x, x', z, \delta)^T_{\mathrm{final}} = \mathbb{M}(x, x', z, \delta)^T_{\mathrm{initial}} \tag{1}$$

where the transfer matrix is

$$\mathbb{M} = \begin{pmatrix} 0 & L_c/3 & \kappa L_s & \eta + \kappa\xi L_s \\ 0 & 0 & \kappa & \kappa\xi \\ \kappa\xi & \eta + \kappa\xi L_s & L_c\kappa^2\xi/6 & L_c^2\kappa^2\xi^2/6 \\ \kappa & \kappa\xi L_s & L_c\kappa^2/6 & L_c\kappa^2\xi/6 \end{pmatrix} \tag{2}$$

and

$$L_s = L + L_{bc} + \frac{L_c}{3}$$

$$L = \frac{2L_b\cos\alpha + L_{bb}}{\cos^2\alpha}$$

$$\eta = \frac{(2L_b\cos^2\alpha - 2L_b\cos\alpha - L_{bb}\sin^2\alpha)}{(\sin\alpha\cos^2\alpha)}$$

$$\xi = \frac{L_{bb}\sin^3\alpha + 2LB\sin\alpha - 2\alpha L_b\cos^2\alpha}{\sin\alpha\cos^2\alpha}$$

* coleman@radiasoft.net

ISBN: 978-3-95450-232-5 ISSN: 2673-7000 doi:10.18429/JACoW-NAPAC2022-MOPA50

and α is the bending angle, L_b is the length of the dipole magnet, L_{bb} is the distance between dipoles, L_{bc} is the distance between the dipole and the TDC, L_c is the length of the TDC, η is the dispersion of the dog-leg, and κ is the deflecting cavity kick strength [7].

Assuming the ideal initial distribution, the transfer matrix yields:

$$(0, 0, \kappa\xi x_0, \kappa)^T = \mathbb{M}(x_0, 0, 0, 0)^T . \quad (3)$$

Extending this to a case with i bunchlets, initial coordinates $\vec{X}_{\text{in.}} = (x_i, 0, 0, 0)$, the transfer matrix yields the final coordinates $\vec{X}_{\text{fin.}} = (0, 0, \kappa\xi x_i, \kappa)$, so a set of discrete horizontally spaced bunchlets entering the EEX will be transformed longitudinally.

SIMULATIONS

The beam optics and propagation was simulated with the OPAL code [13]. The simulations were performed in a piecewise manner using the OPAL-t forward propagation capability to study each section of the AWA before simulating end-to-end. Simulations were first performed of horizontally spaced electron bunchlets entering the EEX using the lattice of the EEX beamline in order to validate that emittance exchange occurred with our beamline parameterization. Secondly, forward simulations were performed to propagate discrete bunchlets from the cathode surface. A synthetic dataset was generated consisting of three rectangular bunchlets, spaced horizontally, consisting of macroparticle electrons distributed uniformly across each emitting surface. The initial momentum distributions were uniformly distributed. These simulations revealed the Larmor rotation of the feature pattern in the solenoid sections of the AWA beamline upstream of the EEX. Next, a pattern was generated that accounted for the rotation induced by the solenoids so that the bunchlets were horizontally spaced at the EEX entrance. Finally, this feature pattern was validated with end-to-end simulations.

The initial pattern consisted of three 1 mm × 1 mm square features with the center of the middle bunchlet at $(x, y) = (0, 0)$ and the other two spaced symmetrically about it. The total simulated charge across all three bunchlets is 200 pC. This relatively large size was chosen to minimize the effects of space charge within the gun and to allow the bunchlets to remain discrete. By shrinking this feature down to 2 µm × 2 µm, we can see in Fig. 1 that space charge effects drive a significant expansion of the transverse bunchlet size, leading to poorer separation at the EEX exit.

The center-to-center spacing of the two other bunchlets was varied to explore the relationship between the cathode feature spacing and the longitudinal spacing at the EEX exit. We found that the longitudinal spacing at the exit of the EEX is linear with respect to the center-to-center spacing of the emitter shapes at the gun cathode surface. This relationship is preserved across a range of cathode feature sizes, as shown in Fig. 2.

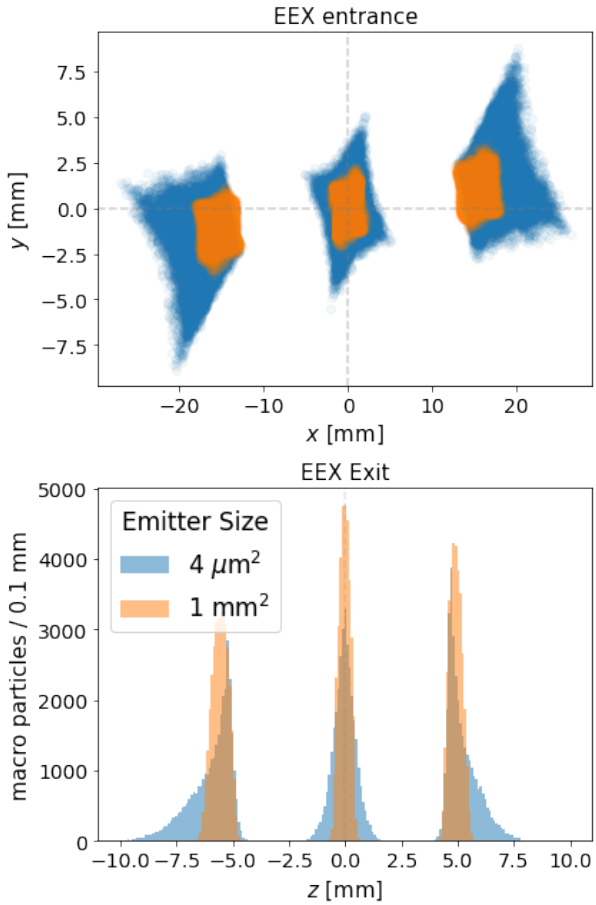

Figure 1: A comparison of simulated cathode features of sizes 1 mm^2 and 4 µm^2 and their transverse distribution at the EEX entrance, as well as the resulting longitudinal distribution at the EEX exit. In both cases the cathode features were initially separated by 0.5 mm.

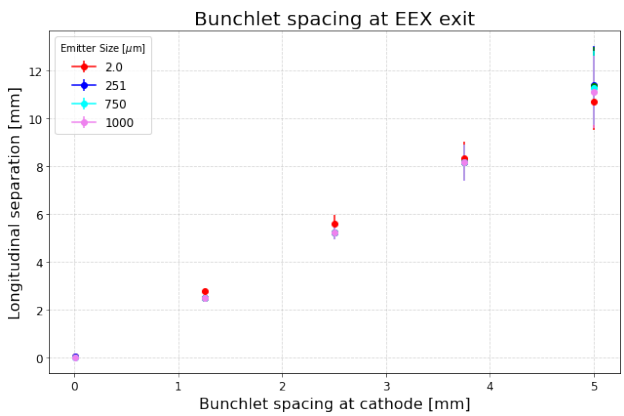

Figure 2: The longitudinal/temporal spacing of the bunchlets exiting the EEX beamline is determined by the transverse spacing of the features on the cathode surface. The longitudinal separation is preserved for many different cathode feature sizes, here described by the edge length of square features.

ISBN: 978-3-95450-232-5 ISSN: 2673-7000 doi:10.18429/JACoW-NAPAC2022-MOPA50

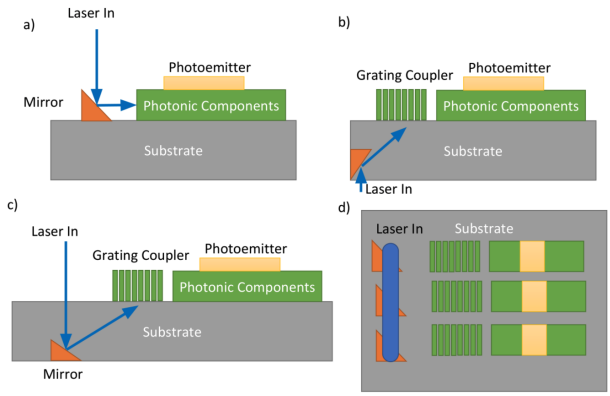

Figure 3: Possible methods for coupling the 262 nm drive laser into an IPS device installed in the gun.

IPS DESIGN

IPS devices generally treat light in an analogous way to electrons in an integrated circuit. There are many design considerations for an IPS device so that it could couple in laser light while it is installed in the AWA gun. The existing laser could be coupled into an IPS waveguide using a mirror and a normally incident laser. Alternatively, grating couplers could be used to take in a laser at an oblique angle (Fig. 3), or from behind.

The IPS photoemitter layer needs to be very thin ($\approx$ 10 nm) so that the electrons can both absorb the evanescently coupled light and also transport to the emitting surface very fast. The depth of the IPS waveguide layer depends on the laser wavelength and also the size of the emittance features, to ensure even power distribution between the three patches and high efficiency. If the waveguide is too thin then the first emitter feature absorbs all of the energy. If it is too thick, then the coupling is very inefficient across all three emitter features. One possible resolution to this is to manipulate the laser so that it can couple in to each emitter feature independently through mirrors and gratings (Fig. 3d).

The initial 1 mm × 1 mm emitter features considered in OPAL simulations are too large for FDTD simulations, however the existing IPS tools are designed for features on the order of tens of microns. Our follow-up OPAL simulations indicate that the smaller emitter features will likely be successful at producing discrete longitudinal bunchlets at this scale.

CONCLUSION

We have shown that Integrated Photonics Systems can be used in conjunction with an emittance exchange beamline to produce tailored longitudinal bunch trains, for driving structure wakefield accelerators or for other purposes, with high wall plug efficiency and transformer ratio. We have also shown how the properties of the EEX beamline can be used to engineer a cathode pattern giving a desired longitudinal distribution at the exit of the EEX.

We have shown that current IPS technology can create the emitter patterns required for THz-scale drive bunches in a structure wakefield accelerator. It is also feasible to couple laser light in to an IPS device while it is installed in a gun.

The IPS techniques described here relatively simple compared to the state-of-the-art. There is great promise for the combination of IPS devices and electron guns for a number of advancements outside of structure wakefield accelerators. These include shapes not achievable with intercepting masks, such as annular beams.

ACKNOWLEDGMENTS

This work is supported by the U.S. Department of Energy, Office of Science, Office of High Energy Physics, under Award Numbers DE-SC0021681 and DE-SC0021213.

REFERENCES

[1] A. Zholents *et al.*, "A preliminary design of the collinear dielectric wakefield accelerator," *Nucl. Instrum. Methods A*, vol. 829, pp. 190–193, 2016, EAAC 2015. doi:10.1016/j.nima.2016.02.003

[2] B. D. O'Shea *et al.*, "Observation of acceleration and deceleration in gigaelectron-volt-per-metre gradient dielectric wakefield accelerators," *Nature Communications*, vol. 7, no. 1, p. 12 763, 2016. doi:10.1038/ncomms12763

[3] J. Picard *et al.*, "Generation of 565 mw of *X*-band power using a metamaterial power extractor for structure-based wakefield acceleration," *Phys. Rev. Accel. Beams*, vol. 25, no. 5, p. 051 301, 2022. doi:10.1103/PhysRevAccelBeams.25.051301

[4] G. Ha *et al.*, "Precision control of the electron longitudinal bunch shape using an emittance-exchange beam line," *Phys. Rev. Lett.*, vol. 118, no. 10, p. 104 801, 2017. doi:10.1103/PhysRevLett.118.104801

[5] Q. Gao *et al.*, "Observation of high transformer ratio of shaped bunch generated by an emittance-exchange beam line," *Phys. Rev. Lett.*, vol. 120, no. 11, p. 114 801, 2018. doi:10.1103/PhysRevLett.120.114801

[6] M. Cornacchia and P. Emma, "Transverse to longitudinal emittance exchange," *Phys. Rev. ST Accel. Beams*, vol. 5, no. 8, p. 084 001, 2002. doi:10.1103/PhysRevSTAB.5.084001

[7] G. Ha *et al.*, "Initial EEX-based Bunch Shaping Experiment Results at the Argonne Wakefield Accelerator Facility," in *Proc. IPAC'15*, Richmond, VA, USA, May 2015, pp. 2575–2577. doi:10.18429/JACoW-IPAC2015-WEPWA035

[8] W. S. Graves, F. X. Kärtner, D. E. Moncton, and P. Piot, "Intense superradiant x rays from a compact source using a nanocathode array and emittance exchange," *Phys. Rev. Lett.*, vol. 108, no. 26, p. 263 904, 2012. doi:10.1103/PhysRevLett.108.263904

[9] C. Jing *et al.*, "Observation of enhanced transformer ratio in collinear wakefield acceleration," *Phys. Rev. Lett.*, vol. 98, no. 14, p. 144 801, 2007. doi:10.1103/PhysRevLett.98.144801

ISBN: 978-3-95450-232-5 ISSN: 2673-7000 doi:10.18429/JACoW-NAPAC2022-MOPA50

[10] C. Jing *et al.*, "Increasing the transformer ratio at the Argonne Wakefield Accelerator," *Phys. Rev. ST Accel. Beams*, vol. 14, no. 2, p. 021 302, 2011. doi:10.1103/PhysRevSTAB.14. 021302

[11] P. Emma, Z. Huang, K.-J. Kim, and P. Piot, "Transverse-to-longitudinal emittance exchange to improve performance of high-gain free-electron lasers," *Phys. Rev. ST Accel. Beams*, vol. 9, p. 100 702, 2006. doi:10.1103/PhysRevSTAB.9. 100702

[12] P. Piot *et al.*, "Commissioning of a 1.3-GHz Deflecting Cavity for Phase-Space Exchange at the Argonne Wakefield Accelerator," in *Proc. IPAC'12*, New Orleans, LA, USA, May 2012, pp. 3350–3352. https://jacow.org/IPAC2012/papers/THPPC031.pdf

[13] A. Adelmann *et al.*, "OPAL a Versatile Tool for Charged Particle Accelerator Simulations," *arXiv e-prints*, 2019. doi: 10.48550/arxiv.1905.06654